

Reversing the Cytotoxicity of Bile Acids by Supramolecular Encapsulation

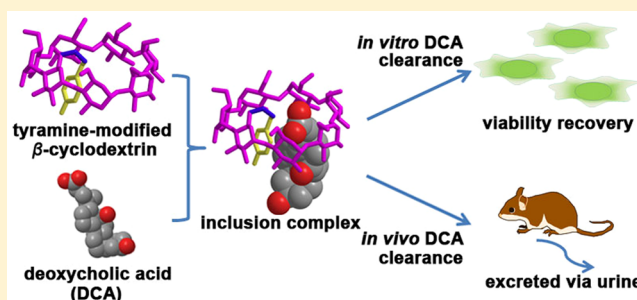
Ying-Ming Zhang,[†] Xun Xu,[†] Qilin Yu,[†] Yao-Hua Liu,[†] Yu-Hui Zhang,[†] Li-Xia Chen,[†] and Yu Liu^{*,†,‡,§}

[†]Department of Chemistry, State Key Laboratory of Elemento-Organic Chemistry, Nankai University, Tianjin 300071, P. R. China

[‡]Collaborative Innovation Center of Chemical Science and Engineering, Tianjin 300071, P. R. China

S Supporting Information

ABSTRACT: Supramolecular encapsulation has been developed into a powerful tool in clearance of toxic substances and hazardous waste from living body and external environments. Herein we tested the special efficacy of tyramine-modified β -cyclodextrin (**1**) in inhibiting and reversing of the inherent cytotoxicity of deoxycholic acid (DCA). The decarboxylation from tyrosine to tyramine in **1** is crucial to the mutual electrostatic communication, ultimately leading to great enhancement in binding affinity and molecular selectivity toward bile acids. As a result, the DCA-mediated cytotoxicity could be largely eliminated by the biocompatible **1**. Meanwhile, the excess DCA could be rapidly excreted by **1** via rat urinary clearance, thus facilitating the decrease of DCA concentration in blood. This study presents a proof of principle that the supramolecular encapsulation with functional cyclodextrin derivatives can efficiently modulate the cell progression and remove the cytotoxic DCA, which provides a practical approach to prevent or treat bile acid-involved diseases.



INTRODUCTION

Bile acids (BAs), a group of important steroids *in vivo*, have been subject to growing interest, primarily due to their various physiological roles and their involvement in pathological processes.¹ The BA-involved biological functions contain two strikingly different aspects; on one hand, BAs as the major organic solutes of bile can be secreted into the duodenum through the bile canaliculi and bile ducts, eventually facilitating the intestinal absorption of dietary lipids and fat-soluble vitamins; on the other hand, the intracellular accumulation of potentially toxic endogenous BAs can lead to severe cholestatic liver injury² and the long-term elevated levels of circulating BAs are identified as risk factors for the development of hepatocellular carcinoma.³ Although the mechanisms by which the amphiphilic BAs contribute to these pathologic conditions are still being investigated, it is absolutely imperative to efficiently remove excessive BAs from their site of action and maintain the metabolism of BAs at normal rate; however, presently alteration of BA profiles and secretion represents a major clinical issue and there is a relative paucity of studies on the rapid and efficient removal of BAs engineered at a molecular level.

Nowadays, supramolecular encapsulation by an exogenous macrocyclic receptor has exerted more powerful influence over modern nanomedicine and consequently exhibited a highly curative effect toward a wide range of diseases.^{4–11} In particular, cyclodextrins (CDs), a class of biocompatible cyclic oligosaccharides with six to eight D-glucopyranose units, are capable of forming stable host–guest complexes with various lipophilic

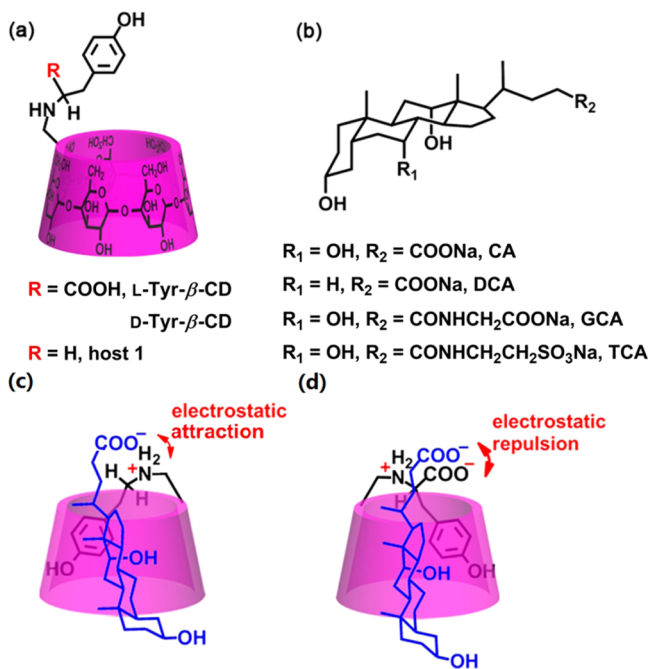
agents, such as steroids.¹² To date, CD treatments have been successfully implemented in the removal of many toxic substances from animal models and human body and largely circumvented the undesired side effects, thereby exhibiting noninvasive therapeutics for clinical use, e.g., reversing neuromuscular blockers in anesthesia,^{13,14} eliminating lipofuscin bisretinoids from retinal pigment epithelium,¹⁵ and reducing free cholesterol from lysosomal storage organelles^{16,17} and atherosclerotic lesions.¹⁸ Motivated by these fascinating results and our ongoing interest concerning the molecular recognition and biological application on water-soluble macrocycles,^{19–22} we can hypothesize that supramolecular encapsulation with functionalized CDs would lead to the reversal of BA's inherent cytotoxicity both *in vitro* and *in vivo*.

We have previously demonstrated that the steroid skeleton of deoxycholic acid (DCA) could be deeply penetrated into the cavity of D-tyrosine-modified β -CD, thus making the hydrophilic carboxylate tail close to the tyrosine group (Scheme 1a and Scheme 1b).²³ This binding geometry subsequently resulted in an enhanced binding ability and selectivity toward the examined bile salts. After scrutinizing the host–guest complex structures, we may suppose that the molecular binding strength in this CD-based molecular recognition system would be further improved if the carboxylate moiety was removed from the side arm of tyrosine because unfavorable COO[−]...COO[−] electrostatic repulsion may occur between the

Received: October 18, 2016

Published: April 11, 2017

Scheme 1. Chemical Structures of (a) Host **1** and Tyr- β -CDs and (b) Four Types of Selected BAs (CA, DCA, GCA, and TCA)^a



^a**1** was synthesized by one-step reaction between tyramine and 6-OTs- β -CD in triethanolamine, and BAs were classified with different hydrophilic tails in length. Plausible molecular binding modes of (c) **1**-DCA and (d) Tyr- β -CD-DCA complexes under physiological condition. There was favorable electrostatic attraction between tyramine's ammonium site and DCA's carboxylate tail, whereas unfavorable electrostatic repulsion may occur between the carboxylate groups of tyrosine and DCA.

carboxylate groups of tyrosine and bile salts, which could further impede the $\text{NH}_2^+\cdots\text{COO}^-$ electrostatic attraction with the adjacent secondary amino group in tyrosine (Scheme 1c and Scheme 1d).²⁴ To test this hypothesis, in this work, the tyramine-modified β -CD (**1**) was synthesized and four of the

most frequently encountered bile salts, namely, the sodium salts of cholic acid (CA), deoxycholic acid (DCA), glycocholic acid (GCA), and taurocholic acid (TCA), were employed to investigate the decarboxylation effect in the molecular binding process with BAs (Figures S1–S3, Supporting Information).²⁵ Physiologically, the primary CA can be 7α -dehydroxylated by colonic bacteria to produce the secondary DCA, and the latter is highly cytotoxic and responsible for the development and pathogenesis of cholestatic liver diseases and related colon cancers.²⁶ Moreover, when conjugated to the amino acids glycine and taurine, it is known that GCA and TCA become more hydrophilic and can counteract the cytotoxic properties of hydrophobic BAs.¹ The molecular binding strength and modes as well as the reversal and removal efficiency of **1** toward DCA were systematically investigated, as described below.

RESULTS AND DISCUSSION

Decarboxylation Effect in Molecular Recognition Process.

After validating the 1:1 binding stoichiometry by Job analysis (Figure S4, Supporting Information), the thermodynamic parameters were evaluated by means of isothermal titration calorimetry (ITC, Figure 1) and the results were listed in Table 1 (Figures S5–S8, Supporting Information). Compared to the previously reported results performed in pure phosphate buffer solution (PBS),²³ the complex stability constant (K_c) was sharply decreased because the hydrophobic interaction was weakened to a great extent in aqueous–organic medium (3% DMSO–PBS mixed solution). Thermodynamically, the molecular recognition process was dominantly governed by the enthalpic gains ($\Delta H^\circ < 0$) and the negative entropic loss ($\Delta S^\circ < 0$). The enthalpic gain was attributed to the combined effect of the hydrophobic and hydrogen-bonding interactions, while the supramolecular complexation of steroid rings makes the accommodated guest molecules more immovable in the β -CD's cavity and this conformational fixation overwhelms the electrostatic desolvation effect to eventually give unfavorable entropic loss.²⁷ It is also noted that this enthalpy-driven intermolecular complexation with tyrosine- and tyramine-modified β -CDs depends to a large degree on the BA's polar tails. That is, the complex

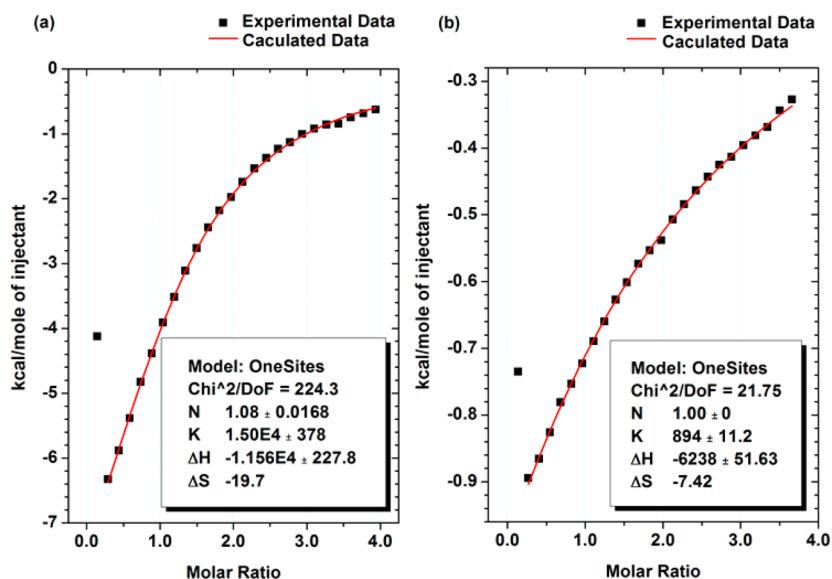


Figure 1. ITC isotherms for the titration of (a) **1**-DCA and (b) **1**-TCA complexation in 3% DMSO–phosphate buffer solution at 25 °C.

Table 1. Complex Stability Constants (K_S , M^{-1}), Standard Free Energy (ΔG° , $\text{kJ}\cdot\text{mol}^{-1}$), Enthalpy (ΔH° , $\text{kJ}\cdot\text{mol}^{-1}$), and Entropy Changes ($T\Delta S^\circ$, $\text{kJ}\cdot\text{mol}^{-1}$) for 1:1 Inclusion Complexation of Host CDs with Bile Salts in 3% DMSO–Phosphate Buffer Solution (pH 7.2, $I = 0.1$) at 25.00 °C

guest	host	K_S	ΔG°	ΔH°	$T\Delta S^\circ$
CA	β -CD	1635 ± 45	-18.3	-27.7 ± 0.1	-9.4
	L-Tyr- β -CD	400 ± 7	-14.9	-36.9 ± 0.2	-22.1
	D-Tyr- β -CD	4650 ± 76	-20.5	-37.0 ± 0.7	-16.5
	1	11800 ± 500	-23.2	-44.1 ± 0.5	-21.0
DCA	β -CD	2150 ± 80	-19.0	-32.0 ± 0.0	-13.0
	L-Tyr- β -CD	627 ± 25	-15.9	-39.6 ± 0.6	-23.7
	D-Tyr- β -CD	4050 ± 56	-20.9	-45.6 ± 0.3	-24.7
	1	15650 ± 650	-23.9	-46.6 ± 1.7	-22.7
GCA	β -CD	1225 ± 5	-17.6	-26.6 ± 0.1	-9.0
	L-Tyr- β -CD	210 ± 5	-13.3	-31.7 ± 0.8	-18.0
	D-Tyr- β -CD	697 ± 25	-16.2	-22.9 ± 0.5	-6.7
	1	1500 ± 40	-18.3	-34.1 ± 1.9	-15.8
TCA	β -CD	1135 ± 5	-17.4	-23.6 ± 0.1	-6.1
	L-Tyr- β -CD	206 ± 1	-13.2	-24.7 ± 0.4	-11.5
	D-Tyr- β -CD	576 ± 23	-15.8	-18.6 ± 0.4	-2.9
	1	888 ± 6	-16.8	-26.2 ± 0.1	-9.4

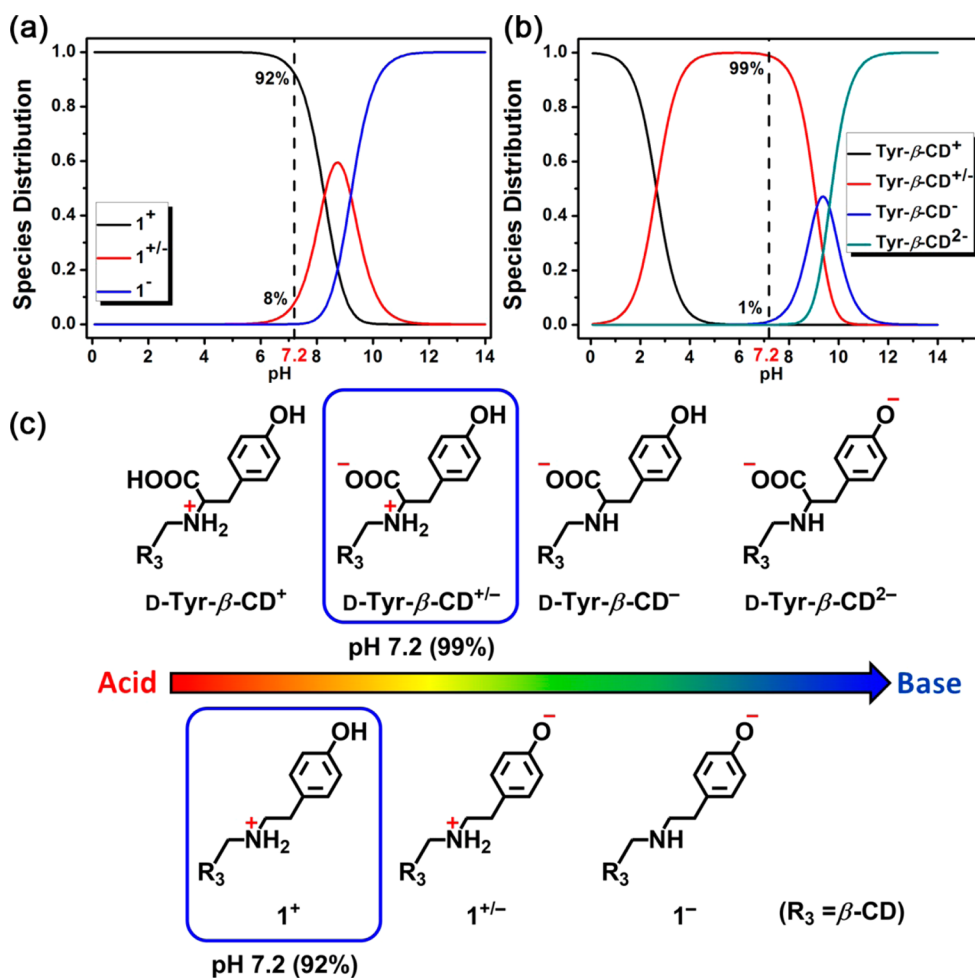


Figure 2. pH-dependent species distribution results of (a) host **1** and (b) D-Tyr- β -CD to demonstrate the decarboxylation effect in the molecular recognition process. The distributions were obtained using the calculated pK_a values by potentiometric titration. (c) Molecular structures in different protonation and deprotonation states derived from the pK_a values of host **1** and D-Tyr- β -CD. The dominant species in D-Tyr- β -CD and host **1** at pH 7.2 are indicated in blue square.

stability constants (K_S) inversely decreased with the substituent length elongating from carboxylate to taurine, with a maximum in the **1**-DCA complex, indicating that the hydrophobic

encapsulation with β -CD's cavity is not sufficient to form a stable host-guest complex and the synergetic cooperativity between the tyramine side arm and BA's hydrophilic tails is also

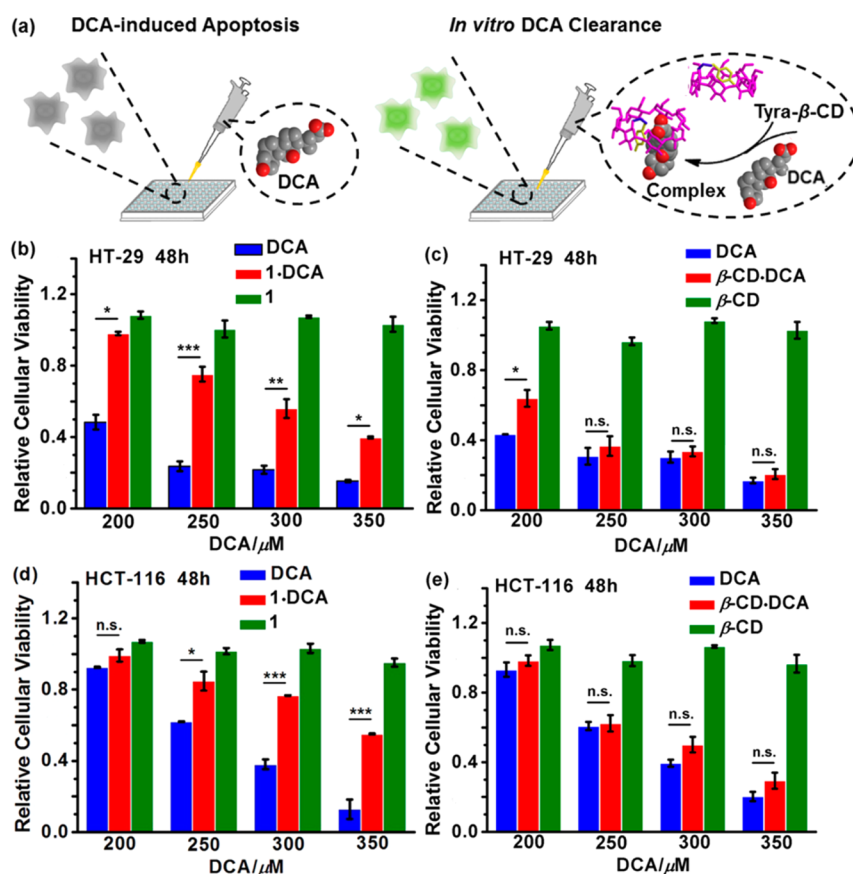


Figure 3. In vitro experiments to evaluate the removal capacity of **1** toward DCA. (a) Schematic illustration of the clearance of DCA by **1** in different cell lines. Relative cellular viability of (b, c) HT-29 and (d, e) HCT-116 cells upon addition of DCA, **1**, native β -CD, and their corresponding inclusion complexes after 48 h. Statistically significant differences are indicated with asterisks ((***) $p < 0.001$, (**) $p < 0.01$, (*) $p < 0.05$, and n.s., not significant). Note that through a calculation based on the binding constants, more than 90% of DCA was converted to 1-DCA inclusion complex, whereas the inclusion efficiency of native β -CD-DCA complex was lower than 60% under the same experimental conditions.

indispensable to enhance the whole binding affinity of **1** with CA and DCA. Moreover, the cross-peaks in ROESY (rotating frame nuclear Overhauser effect spectroscopy) spectrum of 1-DCA complex further corroborated that the DCA's steroid skeleton and the pendent tyramine substituent were concurrently included in the β -CD's cavity (Figure S9, Supporting Information).

Taking the pK_a values of **1** ($pK_{a,1} = 8.27$ and $pK_{a,2} = 9.20$ in Figure 2a) and D-Tyr- β -CD ($pK_{a,1} = 2.65$, $pK_{a,2} = 9.11$, and $pK_{a,3} = 9.62$ in Figure 2b) into account, it is found that under physiological conditions at pH 7.20, the secondary amino group of tyramine is predominantly protonated species in **1** (92%), whereas the zwitterionic structure (both protonation at amino group and deprotonation at carboxyl group) could be exclusively formed in D-Tyr- β -CD (99%, Figure 2c). Therefore, it is rationalized that lacking the carboxyl group, it allows a sufficiently close approach of the protonated amino site in **1** to the exposed carboxylate moiety in bile salts mediated by the supramolecular encapsulation with β -CD's cavity (Scheme 1c and Scheme 1d). Therefore, from the benefit of the additional electrostatic attraction between the protonated amino site and the hydrophilic tail with appropriate molecular length, ITC results showed that CA and DCA gave the strongest binding stability with **1** that reached up to 10^4 M $^{-1}$ order of magnitude in water. More significantly, as can be seen from Table 1, excellent host and guest selectivity was achieved as 18 and 25 ($K_{s_{DCA}}^1/K_{s_{TCA}}^1 = 18$ and $K_{s_{DCA}}^1/K_{s_{DCA}}^{L-Tyr-\beta-CD} = 25$), respectively,

both of which successfully break the former record and are believed as one of the best results in the BA-based molecular recognition systems with monomeric CD derivatives.^{12,23} Furthermore, the binding of DCA with **1** and L-Tyr- β -CD was also examined by Gaussian 09 calculations (Figure S10, Supporting Information). As compared to L-Tyr- β -CD-DCA complex, the binding energy (ΔE) of DCA with **1** was much larger and there were relatively shorter atomic distances between the hydrogen atom of ammonium site and the oxygen atom of carboxylate site in 1-DCA complex. These results suggested that the 1-DCA inclusion complexation is more stable, which is consistent with the thermodynamic parameters obtained by microcalorimetric titrations.

Inhibition Effect of **1** toward Cytotoxic DCA in Vitro.

As compared to the low-cytotoxic GCA and TCA, the highly selective and affinitive binding of **1** toward DCA enabled us to further explore its potential capacity in modulating cell progression (Figure 3a). In our case, two human colorectal cancer cell lines (HT-29 and HCT-116) were employed as model cells because both of them possessed good sensitivities to DCA-induced cytotoxicity.²⁸ The safety of **1** was preliminarily evaluated by measuring the cellular viability of these two cell lines. After incubation at different physiologically relevant concentrations from 10 to 500 μ M individually for 48 h, the cellular viability in **1** group was statistically equivalent to that in the blank group, indicating that host **1** was practically nontoxic and highly biocompatible (Figure S11, Supporting

Information). Moreover, when DCA was added in HT-29 and HCT-116 cells, the dose-dependent cytotoxicity was clearly observed in the range of 200–350 μM . In keen contrast, the cellular viability could be dramatically recovered in the presence of **1** under the same experimental conditions (Figure 3b and Figure 3d). Taking the concentration of HT-29 cells at 200 μM as an example, the relative cellular viability sharply declined after incubation with DCA for 48 h (48%), but **1** exerted a great anticytotoxicity effect and the corresponding viability was comparable to the blank group (98%). Meanwhile, the morphological characteristics of the selected cell lines were also consistent with the results obtained from the cytotoxicity experiments (Figures S12 and S13, Supporting Information). Furthermore, after preincubation with **1** for 4 h, the DCA-induced cytotoxicity was largely eliminated in the HT-29 and HCT-116 cell lines, which basically resembled the viability recovery in the 1-DCA complex groups, suggesting that the addition sequence could not dramatically affect the inhibitory ability of **1** (Figure S14, Supporting Information).

In addition, native β -CD, L- and D-Tyr- β -CDs were used as the references to demonstrate the superiority of **1** in preventing and reversing the cell death. The cellular toxicity tests showed that in the HCT-116 cell line, the cellular viability stayed at a lower stage after incubation with native, L- or D-Tyr- β -CDs for 48 h, especially at higher concentration of DCA (Figures 3e and S15b in the Supporting Information). As for the HT-29 cell line, although the relative cell viability of D-Tyr- β -CD-DCA complex was comparable to that of 1-DCA complex, the inhibitory effect was seriously reduced in the case of native β -CD and L-Tyr- β -CD groups under the same experimental condition, which was attributed to their much weaker inclusion complexation (Figures 3c and S15a in the Supporting Information). In one word, this series of cellular experiments jointly demonstrate that at each concentration of DCA, host **1** always showed satisfactory reversal capacity as compared to other CD derivatives and the supramolecular encapsulation can efficiently prevent the undesirable cytotoxicity from DCA attack, ultimately leading to a remarkable enhancement in cellular viability (Figure 4).

To gain more insight into the efficient clearance of DCA by host **1**, the luminescence- and fluorescent-based assays were exploited to study the inhibition mechanism in the supramolecular encapsulation process. First, annexin-V-FITC/propidium iodide (PI) staining was performed using flow cytometry (FCM), and normal cells were observed in the groups of DCA, **1**, and 1-DCA complex at 300 μM DCA, thus excluding the possibility of DCA-induced apoptosis or necrosis at the relatively low concentration (Figure S16, Supporting Information). Moreover, considering that the decreased adenosine triphosphate (ATP) levels may have a negative impact on cell growth, we next evaluated the changes in metabolic activity by measuring the intracellular ATP content.²⁹ It was revealed that the treatment with 300 μM DCA in HT-29 and HCT-116 cells for 48 h could significantly reduce the ATP content to 14% and 16% compared to 1-DCA complex in HT-29 and HCT-116 cells, respectively. Comparatively, it is noteworthy that the presence of **1** could greatly recover ATP synthesis in both cell lines under DCA treatment, and the percentage of metabolically active cells present in the treated samples could simultaneously be maintained at a higher level (Figures S17 and S18, Supporting Information). Therefore, in the cellular level, a possible mechanism of toxicity may be proposed that involves inactivity of DCA and repair of ATP

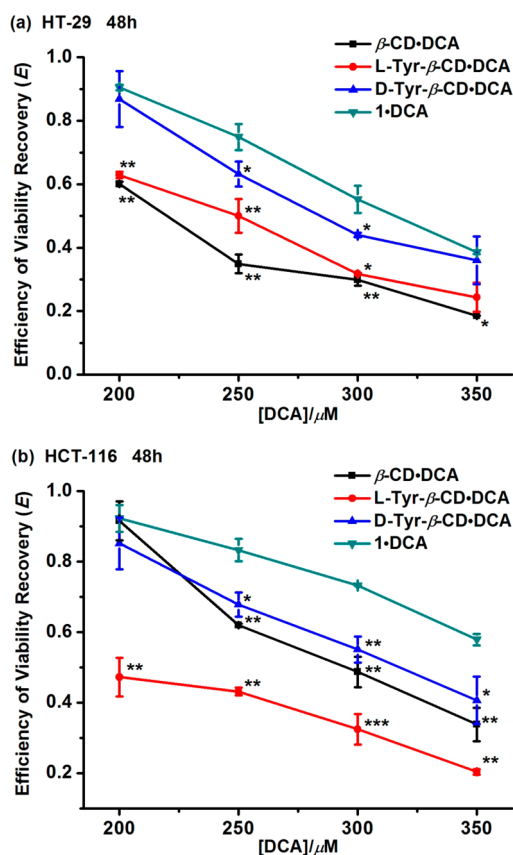


Figure 4. Efficiency of viability recovery (E) of (a) HT-29 and (b) HCT-116 cells upon incubation of DCA-bound inclusion complexes after 48 h. Note that efficiency of viability recovery (E) was defined as $V_{\text{complex}}/V_{\text{host}}$ (V_{complex} and V_{host} are the relative cell viability of host compounds (**1**, native, and L- and D-Tyr- β -CDs) with and without DCA, respectively). These data were extracted from Figures 3 and S15 (Supporting Information). Statistically significant differences are indicated with asterisks (compared to the case of 1-DCA complex at each concentration; (***) $p < 0.001$, (**) $p < 0.01$, and (*) $p < 0.05$).

reduction by supramolecular encapsulation with **1**, ultimately resulting in the enhanced cell viability.

Clearance of Cytotoxic DCA in Vivo. Finally, in vivo experiments were further performed to evaluate the removal capacity of **1** toward DCA. In our case, the total bile acid (TBA) concentrations in mice blood and urine were monitored at different time points after tail intravenous injection of free DCA, **1**, and 1-DCA complex in 120 min (Figure 5a).^{30,31} The TBA concentration in rat blood continuously increased after treatment with 250 μM DCA alone. In contrast, the blood TBA level in the complex-treated group was fairly low under the same time points and started to decline after it reached the peak value at 90 min (Figure 5b). Meanwhile, it was also revealed that DCA could be cleared via urinary excretion more quickly with assistance of **1**; that is, most of DCA was excreted from urine by **1** at 60 min postinjection, whereas no increase in TBA concentration was detected for the DCA group even in a long time of 90 min after tail-vein injection (Figure 5c). Comparatively, only slight fluctuation was observed when treated with **1** alone, indicating that **1** could not interfere with the normal metabolism of bile acids in blood or urine.

Meanwhile, native β -CD, L- and D-Tyr- β -CDs were used as references in the control experiments (Figure S19, Supporting Information). Similar to **1**, no obvious change of TBA

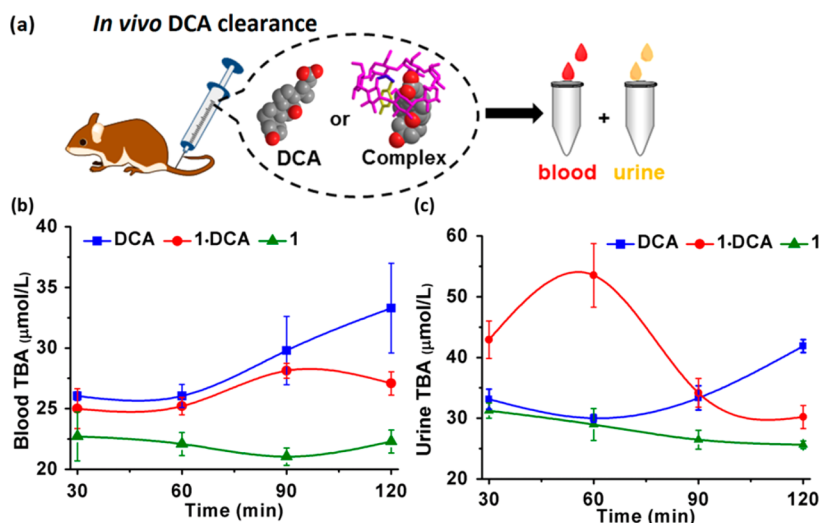


Figure 5. In vivo experiments to evaluate the removal capacity of **1** toward DCA. (a) Schematic illustration of the clearance of DCA by **1** in mice. TBA data of (b) blood and (c) urine after injection with free DCA, **1**, and 1-DCA complex, respectively, in 120 min ($[DCA] = [1] = 250 \mu M$).

concentration was observed in the blood or urine sample when treated by native β -CD, L- or D-Tyr- β -CDs alone, but the TBA concentration in blood continuously increased in 120 min after injection with DCA-bound complexes with native β -CD, L- and D-Tyr- β -CDs. In addition, although DCA could be partially excreted from urine by D-Tyr- β -CD at 60 min, the peak concentration ($45.2 \mu M$) was lower than the one in **1**-treated group ($53.5 \mu M$) under the same experimental conditions. This phenomenon was ascribed to the different binding strength of DCA with **1** and D-Tyr- β -CD as mentioned earlier (Table 1).

Furthermore, the TBA content in liver and gall bladder was also detected using native β -CD and host **1**. As can be seen in Figure S20, host **1** or native β -CD alone could not affect the TBA content in liver, but the treatment of native β -CD-DCA complex still maintained the TBA content at a higher level. Comparatively, the excess DCA could be quickly removed from liver by host **1** in a short time (30–60 min). However, the TBA content in the gall bladder was almost unchanged, due to the fairly high background concentration of endogenous bile acid stored in the mice body.³² Taken together, the in vivo animal experiments demonstrated that the excess DCA could be rapidly excreted through the urinary system of mice due to the strong supramolecular encapsulation with **1**, which was beneficial to maintain the TBA concentration in blood at a normal level. For a comparative purpose, the in vivo removal efficiency of all the employed CD derivatives was summarized in Table 2.

CONCLUSIONS

The present studies provide the first demonstration that the supramolecular encapsulation by **1** could be an effective strategy for the intracellular clearance of toxic BAs. As investigated by microcalorimetric titrations, the decarboxylation of tyrosine can have beneficial effects on the formation of stable supramolecular complex with DCA, thereby leading to the improved binding affinity and molecular selectivity as compared to the corresponding native β -CD and Tyr- β -CDs. In cellular experiments, the DCA-mediated cytotoxicity was eliminated to a great extent upon addition of **1**, and the recovery of cell viability showed a K_S -dependent manner. The curative efficacy of **1** was further evaluated under in vivo conditions, which

Table 2. In Vivo Removal Capacity of Host **1**, Native, and L- and D-Tyr- β -CDs toward DCA

guest	host	TBA content, μM^a	
		blood (after 2 h)	urine (after 1 h)
DCA	none	$33.3 \pm 3.7^{**}$	$30.0 \pm 0.6^{***}$
	native β -CD	$32.2 \pm 2.6^*$	$33.6 \pm 1.3^{***}$
	L-Tyr- β -CD	$32.7 \pm 2.0^*$	$32.2 \pm 3.0^{***}$
	D-Tyr- β -CD	$30.1 \pm 2.0^*$	$45.2 \pm 5.0^*$
	1	27.1 ± 1.0	53.5 ± 5.2

^aThese data were extracted from Figures 5 and S19 (Supporting Information). Statistically significant differences are indicated with asterisks (compared to the case of 1-DCA complex in blood and urine samples; (***) $p < 0.001$, (**) $p < 0.01$, and (*) $p < 0.05$).

demonstrated that the assistance of supramolecular encapsulation of **1** was beneficial for the rapid DCA clearance in rat blood and urine. Considering its convenience in preparation and good discrimination capability toward DCA, we can envision that the removal of endogenous DCA by supramolecular encapsulation with newly modified CDs and known CD derivatives could be developed into a promising therapy for intrahepatic cholestasis and other BA-related diseases.

EXPERIMENTAL SECTION

General. All chemical reagents were commercially available unless noted otherwise. The purity of all CD derivatives was determined to be >95% by a combination of 1H NMR, ^{13}C NMR, and HRMS. The statistical analysis of the data was carried out using the Student's t test. Differences were considered statistically significant if the p value was <0.05.

Mono-6-deoxy-6-N-((4-hydroxyphenyl)ethyl)- β -CD (1). Tyramine (1.0 g) and 6-OTs- β -CD (1.3 g) were dissolved in water (30 mL) and triethanolamine (20 mL), and the resulting mixture was heated at $85^\circ C$ for 24 h with stirring under an argon atmosphere. Then, water was removed by evaporation in vacuo, and then the residue was washed with acetone (300 mL) at least three times to completely remove the excess triethanolamine. The crude solid was purified by column chromatography (silica gel) using n -PrOH/ H_2O /25% $NH_3 \cdot H_2O$ (6:3:0.5, v:v:v) as eluent. After recrystallization from water two times, the target compound **1** was filtered and obtained as white solid (0.15 g, 10%). 1H NMR (400 MHz, DMSO- d_6 , ppm) δ 9.13 (s, 1H), 6.99 (d, 2H), 6.65 (d, 2H), 5.80–5.68 (m, 14H), 4.83 (s,

7H), 4.83–4.46 (m, 6H), 3.66–3.56 (m, 28H), 2.98–2.87 (m, 2H), 2.80–2.61 (m, 4H). ^{13}C NMR (100 MHz, DMSO- d_6 , ppm) δ 155.5, 130.6, 129.6, 115.2, 102.4, 102.2, 83.7, 81.8, 81.7, 73.2, 72.6, 72.2, 60.1, 51.9, 49.5, 35.3. MALDI-ESI: m/z 1254.1515 $[\text{M} + \text{H}]^+$, 1276.4328 $[\text{M} + \text{Na}]^+$, 1292.4074 $[\text{M} + \text{K}]^+$.

Measurements. ITC Measurements. The ITC experiments were performed by an isothermal titration microcalorimeter (VP-ITC, Microcal Inc.) at atmospheric pressure and at 25.00 °C in 3% DMSO–phosphate buffer solution (pH 7.2, $I = 0.1$) to completely dissolve **1**, giving the stability constants (K_s) and the corresponding thermodynamic parameters. A solution of bile salts in a 0.250 mL syringe was sequentially injected with stirring at 300 rpm into a solution of **1** in the sample cell (1.4227 mL volume). The concentrations of **1** and bile salts were used as 0.16 and 3.9 mM, respectively. All the thermodynamic parameters reported in this work were obtained by using the “one set of binding sites” model. Two independent titration experiments were performed to afford self-consistent parameters and to give the averaged values.

Molecular Geometry Calculation. Conformational search was carried out for the 1-DCA and L-Tyr- β -CD-DCA complexes. Geometry optimization and frequency analysis were performed using the B3LYP/6-31G(d) method. All calculations were carried out with Gaussian 09.³³

pK_a Measurement by Potentiometric Titration.³⁴ The pK_a titration experiments were performed with a pH meter (Thermo RION STAR A211). The combination electrode was calibrated with standard solutions (pH = 4.01 and 10.01). The ionic strength was adjusted to 0.1 with 0.1 M KCl. The temperature of the solution was maintained at 25 ± 0.1 °C. The solution of **1** (0.17 mM) was titrated with 0.02 M KOH, and the solution of D-Tyr- β -CD (0.3 mM) was titrated with 0.02 M KOH and 0.02 M HCl, respectively. The dissociation constants of **1** were calculated according to the following eq 1,

$$\frac{\bar{n}_H}{(1 - \bar{n}_H)[\text{H}]} = \frac{1}{K_{a,1}K_{a,2}} \frac{(2 - \bar{n}_H)[\text{H}]}{(1 - \bar{n}_H)} + \frac{1}{K_{a,2}} \quad (1)$$

where $K_{a,1}$ and $K_{a,2}$ are the acidity constants for dissociation of the first and second protons, respectively, and \bar{n}_H is defined as the mean number of bound protons and calculated by using the following eq 2,

$$\bar{n}_H = \frac{2c_1 + [\text{OH}^-] - [\text{H}^+] - [\text{K}^+]}{c_1} \quad (2)$$

where c_1 is the total concentration of investigated **1**, $[\text{OH}^-]$ is the concentration of hydroxyl ions in aqueous solution, $[\text{H}^+]$ is the concentration of the free hydronium ions determined by pH measurement, and $[\text{K}^+]$ is the concentration of added KOH, respectively. Accordingly, the species distribution of protonated **1** (1^+) at the physiological pH (7.20) could be calculated by the following eq 3:

$$[\text{1}^+] = \frac{1}{1 + 10^{\text{pH} - \text{p}K_{a,1}} + 10^{2\text{pH} - \text{p}K_{a,1} - \text{p}K_{a,2}}} \quad (3)$$

The dissociation constants of the basic part of D-Tyr- β -CD were also calculated according to the same method.

Cell Culture. HT-29 and HCT-116 human colorectal cancer cells were purchased from the Peking Union Medical College Hospital (PUMCH, Beijing, China). HT-29 cell lines were cultured in Dulbecco's modified Eagle medium. Nutrient mixture F-12 (DMEM/F-12) and HCT-116 cell lines were cultured in Iscove's mod. Dulbecco's medium (IMDM). Both media were supplemented with 10% fetal bovine serum (FBS) at 37 °C in a humidified 5% CO_2 atmosphere.

MTT Assay. HT-29 and HCT-116 cells were seeded in 96-well plates (5×10^4 cells mL^{-1} , 100 μL per well) for 24 h at 37 °C in 5% CO_2 . Then, the cells were incubated with **1** at different concentrations (10, 50, 100, 250, and 500 μM , respectively) for 24 and 48 h, respectively. The relative cellular viability was determined by the MTT (3-(4,5-dimethylthiazol-2-yl)-2,5-diphenyltetrazolium bromide) assay. All data were presented as the mean \pm standard deviation.

Presto Blue Assay. In vitro cell viability experiments were performed using Presto Blue (Bio Source, Invitrogen, U.K.). Cells were seeded at approximately 5×10^4 cells mL^{-1} in 96-well plates in 100 μL of medium/well. After 24 h, the exponentially growing cell cultures were treated with the different compounds of DCA, **1**, native β -CD, and their corresponding inclusion complexes at different DCA concentrations (200, 250, 300, and 350 μM , respectively). The cells were incubated for 48 h. We also tested the cell viability at the same concentrations after preincubation with **1** for 4 h.

Apoptosis Measurement by Flow Cytometry. HCT-116 cells (5×10^5 cells per well) were seeded in 6-well plates for 24 h. Then, the cells were treated with 300 μM DCA, **1**, 1-DCA complex for 48 h, collected, washed, and then resuspended in 500 μL of binding buffer containing 5 μL of annexin V-FITC and 5 μL of PI. The cells were incubated in the dark for 10 min at 25 °C and then analyzed by the flow cytometer (FCM) (FACSCalibur, BD Biosciences, San Jose, CA, USA).

Determination of ATP Content. ATP content was measured by the ATP assay kit (Beyotime, China) following the instructions of the manufacturer. Briefly, HCT-116 cells and HT-29 cells (1×10^6 cells per mL) were treated by 300 μM DCA, 300 μM **1**, and their corresponding inclusion complexes and washed twice by PBS. The cells were then lysed in a lysis buffer and centrifuged at 1000g for 10 min. The supernatant was mixed with the ATP assay kit reaction buffer. After mixing gently, the luminescence density was detected using a fluorescent microplate reader (Enspire, PerkinElmer, USA) to reflect cellular ATP levels.

In Vivo Total Bile Acid (TBA) Assay. BALB/c female mice were housed under constant temperature (23 ± 1 °C) and controlled humidity (45–65%) and a standard 12 h light/dark cycle. Animals fasted for at least 2 h prior to the experiments. Solutions of DCA, **1**, and 1-DCA complex were prepared in sterile saline solutions (0.9%) at the same concentration of 250 μM (containing 5% DMSO). Mice were randomly divided into four groups ($n = 5$). Each mouse was intravenously injected through the tail vein with 400 μL of the solutions (saline, DCA, **1**, and Tyr- β -CDs and the corresponding complexes with DCA). The treated mice were maintained under the same experimental conditions, and no abnormal behavior or symptom was observed. At the indicated time points (30, 60, 90, and 120 min), the mice blood were taken by removing the eyeball and executed via cervical dislocation, followed by collection of urine. The collected blood samples were centrifuged at 1500 rpm for 5 min to obtain the serum. Meanwhile, the mice were put to death, and the liver and gall bladder were removed for detection of TBA content. The liver was homogenized for 10–20 strokes with a Dounce homogenizer, and the homogenate was then centrifuged to obtain the liver extract. Then, the TBA content in the serum, collected urine, liver extract, and gall bladder was detected using a total bile acid (TBA) kit according to the manufacturer's instructions (Nanjing Jiancheng Bioengineering Institute, China). All mouse experiments were approved by the Institutional Animal Care and Use Committee of Nankai University. All mice have free access to food and water throughout the experiments.

■ ASSOCIATED CONTENT

● Supporting Information

The Supporting Information is available free of charge on the ACS Publications website at DOI: 10.1021/acs.jmedchem.6b01536.

Compound characterization, quantum chemical calculation results (Cartesian coordinates for the optimized structures), and additional figures in the cellular experiments (PDF)

Molecular formula strings and some data (CSV)

■ AUTHOR INFORMATION

Corresponding Author

*Phone: +86-22-23503625. Fax: +86-22-23503625. E-mail: yuliu@nankai.edu.cn.

ORCID 

Yu Liu: 0000-0001-8723-1896

Notes

The authors declare no competing financial interest.

■ ACKNOWLEDGMENTS

We thank the National Natural Science Foundation of China (Grants 21432004, 21472100, and 91527301) for financial support.

■ ABBREVIATIONS USED

I, tyramine-modified β -cyclodextrin; L-Tyr- β -CD, L-tyrosine-modified β -cyclodextrin; D-Tyr- β -CD, D-tyrosine-modified β -cyclodextrin

■ REFERENCES

- (1) Verhaag, E. M.; Buist-Homan, M.; Koehorst, M.; Groen, A. K.; Moshage, H.; Faber, K. N. Hormesis in cholestatic liver disease; preconditioning with low bile acid concentrations protects against Bile acid-induced toxicity. *PLoS One* **2016**, *11*, e0149782.
- (2) Woolbright, B. L.; Dorko, K.; Antoine, D. J.; Clarke, J. I.; Gholami, P.; Li, F.; Kumer, S. C.; Schmitt, T. M.; Forster, J.; Fan, F.; Jenkins, R. E.; Park, B. K.; Hagenbuch, B.; Olyae, M.; Jaeschke, H. Bile acid-induced necrosis in primary human hepatocytes and in patients with obstructive cholestasis. *Toxicol. Appl. Pharmacol.* **2015**, *283*, 168–177.
- (3) Zhang, W.; Zhou, L.; Yin, P.; Wang, J.; Lu, X.; Wang, X.; Chen, J.; Lin, X.; Xu, G. A weighted relative difference accumulation algorithm for dynamic metabolomics data: long-term elevated bile acids are risk factors for hepatocellular carcinoma. *Sci. Rep.* **2015**, *5*, 8984.
- (4) Lazar, A. I.; Biedermann, F.; Mustafina, K. R.; Assaf, K. I.; Hennig, A.; Nau, W. M. Nanomolar binding of steroids to cucurbit[n]urils: selectivity and applications. *J. Am. Chem. Soc.* **2016**, *138*, 13022–13029.
- (5) Ni, M.; Zhang, N.; Xia, W.; Wu, X.; Yao, C.; Liu, X.; Hu, X.-Y.; Lin, C.; Wang, L. Dramatically promoted swelling of a hydrogel by pillar[6]arene–ferrocene complexation with multistimuli responsiveness. *J. Am. Chem. Soc.* **2016**, *138*, 6643–6649.
- (6) Ma, X.; Zhao, Y. Biomedical applications of supramolecular systems based on host–guest interactions. *Chem. Rev.* **2015**, *115*, 7794–7839.
- (7) Simões, S. M. N.; Rey-Rico, A.; Concheiro, A.; Alvarez-Lorenzo, C. Supramolecular cyclodextrin-based drug nanocarriers. *Chem. Commun.* **2015**, *51*, 6275–6289.
- (8) Tian, J.; Zhou, T.-Y.; Zhang, S.-C.; Aloni, S.; Altoe, M. V.; Xie, S.-H.; Wang, H.; Zhang, D.-W.; Zhao, X.; Liu, Y.; Li, Z.-T. Three-dimensional periodic supramolecular organic framework ion sponge in water and microcrystals. *Nat. Commun.* **2014**, *5*, 5574.
- (9) Andrade, B.; Song, Z.; Li, J.; Zimmerman, S. C.; Cheng, J.; Moore, J. S.; Harris, K.; Katz, J. S. New frontiers for encapsulation in the chemical industry. *ACS Appl. Mater. Interfaces* **2015**, *7*, 6359–6368.
- (10) Wang, L.; Li, L.-L.; Fan, Y.-s.; Wang, H. Host–guest supramolecular nanosystems for cancer diagnostics and therapeutics. *Adv. Mater.* **2013**, *25*, 3888–3898.
- (11) Ma, D.; Hettiarachchi, G.; Nguyen, D.; Zhang, B.; Wittenberg, J. B.; Zavalij, P. Y.; Briken, V.; Isaacs, L. Acyclic cucurbit[n]uril molecular containers enhance the solubility and bioactivity of poorly soluble pharmaceuticals. *Nat. Chem.* **2012**, *4*, 503–510.
- (12) Liu, Y.; Wang, K. Thermodynamics of resulting complexes between cyclodextrins and bile salts. In *Thermodynamics—Fundamentals and Its Application in Science*; Morales-Rodriguez, R., Ed.; InTech: Rijeka, Croatia, 2012; pp 305–338.
- (13) Bom, A.; Bradley, M.; Cameron, K.; Clark, J. K.; van Egmond, J.; Feilden, H.; Maclean, E. J.; Muir, A. W.; Palin, R.; Rees, D. C.; Zhang, M.-Q. A novel concept of reversing neuromuscular block: chemical encapsulation of rocuronium bromide by a cyclodextrin-based synthetic host. *Angew. Chem., Int. Ed.* **2002**, *41*, 265–270.
- (14) Adam, J. M.; Bennett, D. J.; Bom, A.; Clark, J. K.; Feilden, H.; Hutchinson, E. J.; Palin, R.; Prosser, A.; Rees, D. C.; Rosair, G. M.; Stevenson, D.; Tarver, G. J.; Zhang, M.-Q. Cyclodextrin-derived host molecules as reversal agents for the neuromuscular blocker rocuronium bromide: synthesis and structure-activity relationships. *J. Med. Chem.* **2002**, *45*, 1806–1816.
- (15) Nociari, M. M.; Lehmann, G. L.; Perez Bay, A. E.; Radu, R. A.; Jiang, Z.; Goicochea, S.; Schreiner, R.; Warren, J. D.; Shan, J.; Adam de Beaumais, S.; Ménand, M.; Sollogoub, M.; Maxfield, F. R.; Rodriguez-Boulan, E. Beta cyclodextrins bind, stabilize, and remove lipofuscin bisretinoids from retinal pigment epithelium. *Proc. Natl. Acad. Sci. U. S. A.* **2014**, *111*, E1402–E1408.
- (16) Rosenbaum, A. I.; Zhang, G.; Warren, J. D.; Maxfield, F. R. Endocytosis of beta-cyclodextrins is responsible for cholesterol reduction in Niemann-Pick type C mutant cells. *Proc. Natl. Acad. Sci. U. S. A.* **2010**, *107*, 5477–5482.
- (17) Tamura, A.; Yui, N. Lysosomal-specific cholesterol reduction by biocleavable polyrotaxanes for ameliorating Niemann-Pick type C disease. *Sci. Rep.* **2014**, *4*, 4356.
- (18) Zimmer, S.; Grebe, A.; Bakke, S. S.; Bode, N.; Halvorsen, B.; Ulas, T.; Skjelland, M.; De Nardo, D.; Labzin, L. I.; Kerkusiek, A.; Hempel, C.; Heneka, M. T.; Hawxhurst, V.; Fitzgerald, M. L.; Trebicka, J.; Björkhem, I.; Gustafsson, J.-Å.; Westerterp, M.; Tall, A. R.; Wright, S. D.; Espevik, T.; Schultze, J. L.; Nickenig, G.; Lütjohann, D.; Latz, E. Cyclodextrin promotes atherosclerosis regression via macrophage reprogramming. *Sci. Transl. Med.* **2016**, *8*, 333ra50.
- (19) Chen, Y.; Liu, Y. Construction and functions of cyclodextrin-based 1D supramolecular strands and their secondary assemblies. *Adv. Mater.* **2015**, *27*, 5403–5409.
- (20) Chen, Y.; Liu, Y. Cyclodextrin-based bioactive nanosupramolecules. *Chem. Soc. Rev.* **2010**, *39*, 495–505.
- (21) Chen, Y.; Zhang, Y.-M.; Liu, Y. Multidimensional nano-architectures based on cyclodextrins. *Chem. Commun.* **2010**, *46*, 5622–5633.
- (22) Liu, Y.; Chen, Y. Cooperative binding and multiple recognition by bridged bis(β -cyclodextrin)s with functional linkers. *Acc. Chem. Res.* **2006**, *39*, 681–691.
- (23) Chen, Y.; Li, F.; Liu, B.-W.; Jiang, B.-P.; Zhang, H.-Y.; Wang, L.-H.; Liu, Y. Thermodynamic origin of selective binding of β -cyclodextrin derivatives with chiral chromophoric substituents toward steroids. *J. Phys. Chem. B* **2010**, *114*, 16147–16155.
- (24) Zhang, Y.-M.; Wang, Z.; Chen, Y.; Chen, H.-Z.; Ding, F.; Liu, Y. Molecular binding behavior of a bispyridinium-containing bis (β -cyclodextrin) and its corresponding [2] rotaxane towards bile salts. *Org. Biomol. Chem.* **2014**, *12*, 2559–2567.
- (25) Hennig, A.; Bakirci, H.; Nau, W. M. Label-free continuous enzyme assays with macrocycle-fluorescent dye complexes. *Nat. Methods* **2007**, *4*, 629–632.
- (26) Katona, B. W.; Rath, N. P.; Anant, S.; Stenson, W. F.; Covey, D. F. Enantiomeric deoxycholic acid: total synthesis, characterization, and preliminary toxicity toward colon cancer cell lines. *J. Org. Chem.* **2007**, *72*, 9298–9307.
- (27) Chen, L.; Zhang, Y.-M.; Liu, Y. Molecular binding behaviors between tetrasulfonated bis(*m*-phenylene)-26-crown-8 and bispyridinium guests in aqueous solution. *J. Phys. Chem. B* **2012**, *116*, 9500–9506.
- (28) Katona, B. W.; Anant, S.; Covey, D. F.; Stenson, W. F. Characterization of enantiomeric bile acid-induced apoptosis in colon cancer cell lines. *J. Biol. Chem.* **2009**, *284*, 3354–3364.
- (29) AshaRani, P. V.; Low Kah Mun, G.; Hande, M. P.; Valiyaveetil, S. Cytotoxicity and genotoxicity of silver nanoparticles in human cells. *ACS Nano* **2009**, *3*, 279–290.
- (30) Shi, H.; Zhang, K.; Mao, X. Effects of cholic acid on the liver in SD rats. *J. Shanghai Jiaotong Univ. (Agric. Sci.)* **1999**, *17* (26–29), 51.

(31) Tian, X.; Sun, J.; Pan, Z.; Li, X.; Hu, Y.; Mao, X. Experimental studies on effects of cholic acid and estrogen loading to liver and gallbladder function in rats. *Jiangsu Med. J.* **2001**, *27*, 420–422.

(32) Debray, D.; Rainteau, D.; Barbu, V.; Rouahi, M.; el Mourabit, H.; Lerondel, S.; Rey, C.; Humbert, L.; Wendum, D.; Cottart, C.-H.; Dawson, P.; Chignard, N.; Housset, C. Defects in gallbladder emptying and bile acid homeostasis in mice with cystic fibrosis transmembrane conductance regulator deficiencies. *Gastroenterology* **2012**, *142*, 1581–1591.

(33) Frisch, M. J.; Trucks, G. W.; Schlegel, H. B.; Scuseria, G. E.; Robb, M. A.; Cheeseman, J. R.; Scalmani, G.; Barone, V.; Mennucci, B.; Petersson, G. A.; Nakatsuji, H.; Caricato, M.; Li, X.; Hratchian, H. P.; Izmaylov, A. F.; Bloino, J.; Zheng, G.; Sonnenberg, J. L.; Hada, M.; Ehara, M.; Toyota, K.; Fukuda, R.; Hasegawa, J.; Ishida, M.; Nakajima, T.; Honda, Y.; Kitao, O.; Nakai, H.; Vreven, T.; Montgomery, J. A., Jr.; Peralta, J. E.; Ogliaro, F.; Bearpark, M.; Heyd, J. J.; Brothers, E.; Kudin, K. N.; Staroverov, V. N.; Keith, T.; Kobayashi, R.; Normand, J.; Raghavachari, K.; Rendell, A.; Burant, J. C.; Iyengar, S. S.; Tomasi, J.; Cossi, M.; Rega, N.; Millam, J. M.; Klene, M.; Knox, J. E.; Cross, J. B.; Bakken, V.; Adamo, C.; Jaramillo, J.; Gomperts, R.; Stratmann, R. E.; Yazyev, O.; Austin, A. J.; Cammi, R.; Pomelli, C.; Ochterski, J. W.; Martin, R. L.; Morokuma, K.; Zakrzewski, V. G.; Voth, G. A.; Salvador, P.; Dannenberg, J. J.; Dapprich, S.; Daniels, A. D.; Farkas, O.; Foresman, J. B.; Ortiz, J. V.; Cioslowski, J.; Fox, D. J. *Gaussian 09*, revision E.01; Gaussian, Inc.: Wallingford, CT, 2013.

(34) Zhang, Y.-M.; Yang, Y.; Zhang, Y.-H.; Liu, Y. Polysaccharide nanoparticles for efficient siRNA targeting in cancer cells by supramolecular pK_a shift. *Sci. Rep.* **2016**, *6*, 28848.